Organic & Biomolecular Chemistry

PAPER

View Article Online
View Journal

Cite this: DOI: 10.1039/c9ob01250h

Sulfonic nucleic acids (SNAs): a new class of substrate mimics for ribonuclease A inhibition†

Dhrubajyoti Datta, Swagata Dasgupta * and Tanmaya Pathak *

Received 30th May 2019,
Accepted 4th July 2019

DOI: 10.1039/c9ob01250h

rsc.li/obc

Sulfonic nucleic acids were identified as inhibitors of ribonuclease A (RNase A). The incorporation of a strongly acidic group (sulfonic, $-SO_3H$) at the 3′-end of pyrimidine nucleosides thymidine and uridine was prompted by the low inhibition constant (K_i) values recorded for carboxymethylsulfonyl ($-SO_2CH_2CO_2H$) and $-CO_2H$ functionalized nucleosides. It was envisaged that the sulfonic acid-modified pyrimidines would bind effectively with the positively charged P_1 site of ribonuclease A. Typical harsh conditions used for SO_3H incorporation were replaced with milder reaction conditions. The uridine analogue showing a K_i value of 0.96 μM elicited a better result than the thymidine-modified inhibitor. Notably, it was also the best result among all modified non-phosphate acidic nucleosides reported and screened so far as RNase A inhibitors.

1. Introduction

Ribonuclease A (RNase A) is used as a model system[1,2–6] for different RNases which are neurotoxic, helminthotoxic and antiviral in nature.[7,8] In the same line, inhibition of angiogenesis is also addressed which leads to the growth of tumor cells[7,8] by angiogenin, one of the members of the RNase super-family. It is because most of these enzymes consist of similar RNA binding subsites termed P_0...P_n, R_0...R_n and B_0...B_n corresponding to phosphate, ribose and nucleobase recognition for the bound RNA, respectively (n is the position of the group with respect to the cleaved phosphodiester bond where n = 1) (Fig. 1). In RNases, the pyrimidine and purine base recognition sites B_1 and B_2 are partially conserved while the phosphate binding P_1 is fully conserved.[9]

Despite the fact that an overwhelming number of reported reversible and mechanism-based inhibitors of RNase A are either phosphate- or pyrophosphate-functionalized nucleotides,[10–15] the design of nucleoside-modified RNase A inhibitors is constantly required to avoid serious limitations of nucleotide-based inhibitors because of their poor cell-permeability and susceptibility towards phosphatases. From a synthetic point of view, the purification of relatively large amounts of these nucleotides is a challenging task owing to their highly polar nature.[9,16–19]

The binding studies of synthetic nucleosides with the active sites of RNase A have resulted in a wealth of valuable information and led to the identification of new classes of inhibitors.[20–32] While co-crystal structures provided the unambiguous proof[21,27,29] of interactions between the amino acid residues of RNase A[1] and inhibitors at the atomic level, the screening of a series of nucleosidic and non-nucleosidic inhibitors further confirmed the active site topology of the enzyme. In an attempt to generate substrate-like inhibitors, various modified dinucleosides[25,26,29,31,33] and disaccharides[32] were synthesized which are able to accommodate themselves into the crescent-shaped active site of the enzyme. Among various sets of nucleoside-modified RNase A inhibitors synthesized to date, polar and acidic nucleosides inhibited the ribonucleolytic activity to a larger extent compared to the corresponding basic and/or neutral congeners. The perturbation of the active enzyme environment of RNase A during its

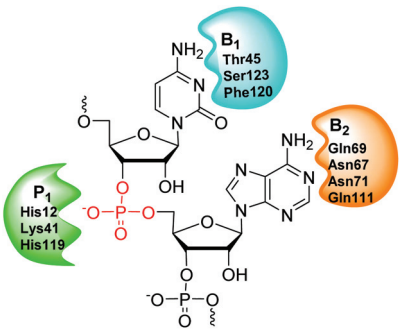

Fig. 1 Pictorial representation of amino acid residues in P_1, B_1 and B_2 subsites of RNase A along with its natural substrate.

Department of Chemistry, Indian Institute of Technology Kharagpur, Kharagpur 721302, India. E-mail: swagata@chem.iitkgp.ac.in, tpathak@chem.iitkgp.ac.in; Fax: +91-3222-255303; Tel: +91-3222-283306, +91-3222-283342

†Electronic supplementary information (ESI) available. See DOI: 10.1039/c9ob01250h

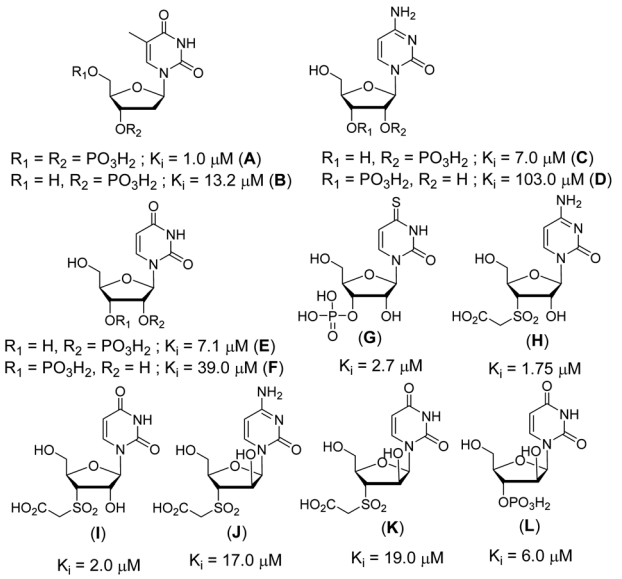

Fig. 2 Representative nucleotidic and acidic nucleosides with low K_i values.

catalytic action[20,33] is effectively exhibited by the inhibitors with low pK_a values.[34] Among the nucleotide monomers, pT-3′-p (**A**), T-3′-p (**B**), C-2′-p (**C**), C-3′-p (**D**), U-2′-p (**E**), U-3′-p (**F**) and 4-thio-U-3′-p (**G**) exhibited K_i values ranging from 1 to 103 μM as inhibitors of RNase A (Fig. 2).[35,36] Among the modified acidic nucleosides tested as RNase A inhibitors in our laboratory, only the 3′-ribo-nucleosides (**H**) and (**I**)[30] resulted in such low K_i values to date, whereas, the arabino analogues **J** and **K** with an "up" configuration of the 2′-hydroxyl group showed reduced inhibitory properties by approximately 8–9 fold (Fig. 2).[28] Nevertheless, arabino-nucleotide ara-U-3′-p (**L**)[35b] exhibited a lower K_i value (Fig. 2) than the corresponding ribo-analogues **F**[35b] and the cytidine derivative **D**.[35a]

Sulfonic acid-modified nucleosides or sulfonic nucleic acids (SNAs) are a lesser known class of modified nucleosides scarcely used for biological studies.[37–41] Since compounds **H–K** having pK_a values of the $-SO_2CH_2COOH$ group around 2.39 ± 0.1 showed reasonably good inhibition, we argued that a nucleoside functionalized with a much stronger acidic group such as $-SO_3H$ (pK_a = −1.9 for methanesulfonic acid[42]) would also show significant RNase A inhibitory properties.[43]

2. Results and discussion

2.1. Synthesis of inhibitors

For the synthesis of sulfonic acid-modified nucleosides milder conditions were developed. Thus, treatment of **1**[34] under prolonged basic conditions of 1 M NaOH solution followed by acidic hydrolysis with 20% TFA in DCM afforded compound **2** in 60% yield over two steps which was confirmed by ^{1}H, ^{13}C NMR and high resolution mass spectroscopy (HRMS). This is the first report of a sulfonic acid group being generated in the absence of typically harsh conditions.[44–47] In order to understand the effect of hydroxyl groups at the 2′-site of nucleosides, another pyrimidine derivative **3**,[28] an arabino-uridine analogue, was chosen and converted to **4** under similar reaction conditions. The sulfonic acid-modified uridine **4** was obtained in moderate yield in two steps (Scheme 1). However, all attempts to synthesize the ribo analogue failed.

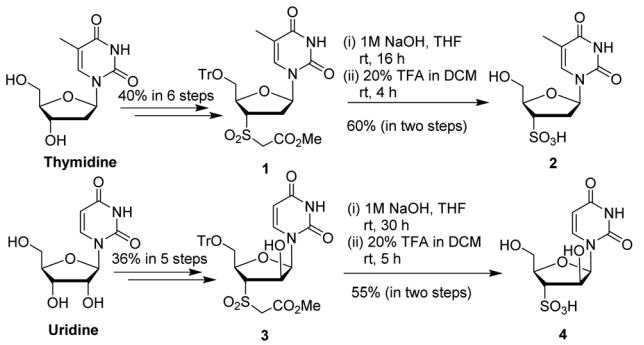

Scheme 1 Synthesis of 3′-thymidine and uridine sulfonic acids **2** and **4**.

2.2. Docking studies

Prevalent bioisosterism between phosphate and sulfate groups owing to their physical and chemical properties[48] prompted us to check the interaction of these two modified nucleosides with the active site amino acid residues of RNase A through *in silico* studies. From the molecular docking studies, it was clear that the hydrogen bonding (H-bonding) possibly between the sulfonate group of **2** and the amino acid residues at the P_1 site of RNase A is the major interaction. Although, the expected interaction of the pyrimidine nucleobase with the B_1 site is completely missing due to the outward movement of nucleobase thymine, it was well compensated for by the H-bonding interactions with another amino acid such as Gln11. The lack of pyrimidine base recognition was evident also for **4** in its docked conformation with RNase A. However, unlike **2**, the nucleobase did not completely shift away from the B_1 site and was held by at least three possible H-bonding interactions by nearby amino acid residues. Thus, both **2** and **4** could accommodate themselves into the active site P_1 of RNase A to replace the substrate and potentially acted as substrate mimics (Fig. 3 and ESI†). There are a greater number of H-bonding interactions with shorter H-bond distances for **4** than those of its thymidine analogue **2** (ESI†). Simultaneously, the number of H-bonding interactions for inhibitors **2** and **4** are more (eight and nine, respectively) than those for the corresponding phosphate analogues (five and eight for **B** and **L**, respectively), which are observed in docking studies (ESI†). For the aforementioned studies, the crystal structure of RNase A (PDB entry: 1FS3) from the Protein Data Bank[49] was used for the docking studies after the subtraction of water molecules and any other ions. The three-dimensional structures of modified nucleosides were generated, energy-minimized and thereafter used for subsequent docking studies. Various types of

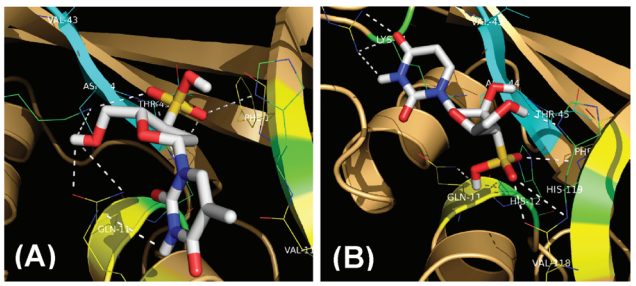

Fig. 3 Docked pose of (A) inhibitor **2** and (B) inhibitor **4** with RNase A where B_1, P_1, and other subsites are highlighted in cyan, green and yellow, respectively.

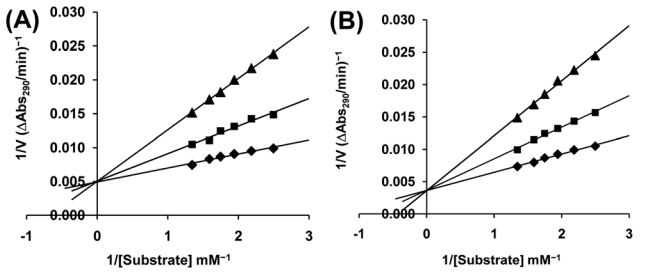

Fig. 5 Lineweaver–Burk plots for inhibition of RNase A by (A) **2** of 6.30 (▲), 3.15 (■), and 0.0 (◆) μM, and (B) **4** of 2.16 (▲), 1.06 (■), and 0.0 (◆) μM with 2′,3′-cCMP as the substrate (0.74–0.40 μM) and an RNase A concentration of 10.0 μM.

molecular interactions between the inhibitor and protein were considered according to Rarey *et al.*[50]

2.3. Biophysical assays

2.3.1. Agarose gel electrophoresis. The inhibitory properties of **2** and **4** were studied qualitatively by agarose gel electrophoresis experiments. The representative agarose gel (Fig. 4) depicted the maximum intensity in lane I due to the presence of only tRNA. Due to the degradation of tRNA by RNase A, the band in lane II was the least intense. Lanes III and IV of each gel contained tRNA and RNase A with increasing concentrations of inhibitor **2**/**4** and therefore were more intense under UV light compared to lane II. As a control experiment, lane V contained a mixture of only the substrate and inhibitor which exhibited an equal intensity of tRNA alone. A similar observation was also noted for inhibitor **4**. This preliminary assay showed equal potency of inhibitors **2** and **4** which was again quantified using the relative intensity of residual tRNA which was visualized under UV light as depicted in the histogram (ESI†).

2.3.2. Enzyme kinetics. To quantify the RNase A inhibition of sulfonic acid-modified nucleosides, enzyme kinetics studies were performed to obtain the inhibition constant (K_i) values. The Lineweaver–Burk plots (Fig. 5) confirmed that this new class of inhibitors of RNase A are competitive and reversible in nature with low micromolar K_i values as mentioned in Table 1. It was observed that the thymidine-modified inhibitor **2** (K_i = 2.08 ± 0.08 μM) was a comparatively weaker inhibitor with respect to its uridine analogue **4** (K_i = 0.96 ± 0.05 μM). The decrease in the K_i value was likely due to the arabino configuration of the sugar ring with the uracil nucleobase for inhibitor **4** which furnished better hydrogen bonding abilities than **2** (Table 1). The results obtained from the kinetics study also confirmed and corroborated the data obtained from the agarose gel-based studies. It was interesting to note that only a few nucleotidic RNase A inhibitors, such as **A** and **G** showed K_i values (1 and 2.7 μM respectively; Fig. 2) which are comparable to those of **2** and **4**. On the other hand among the carboxymethylsulfonyl-modified pyrimidine nucleosides reported from our group, only 3′-ribo-nucleosides **H** and (**I**)[30] resulted in such low K_i values to date. Moreover, the carboxymethylsulfonyl-modified arabino analogues **J** and **K** showed reduced inhibitory properties (Fig. 2) whereas SNA arabino analogue **4** turned out to be a more efficient inhibitor.

Table 1 Inhibition constants (K_i) of inhibitors **2** and **4**

Inhibitor	K_i[a] (μM)
2	2.08 ± 0.08
4	0.96 ± 0.05

[a] Data are the mean ± SD (n = 4).

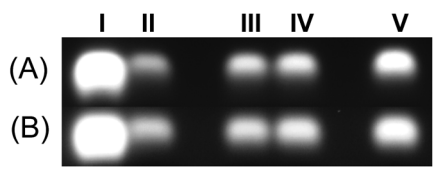

Fig. 4 Agarose gel-based assay for the inhibition of RNaseA. Lane I: tRNA; lane II: tRNA and RNase A; lanes III and IV: tRNA, RNaseA (1 μM) and inhibitors with two different concentrations [0.10 and 0.20 μM, respectively] for (A) inhibitor **4** and (B) inhibitor **2**; lane V: tRNA and (A) inhibitors **4** and (B) **2**, respectively (0.20 μM each).

2.4. Permeability assay

After assessing the inhibitory properties quantitatively from the Lineweaver–Burk plots, we tried to address the cell-permeability issues for these sulfonic acid-functionalized modified nucleosides. For that, we employed the shake flask[28,51] method to understand the octanol/water partition coefficients of these RNase A inhibitors. The data thus obtained were compared (Table 2) to those of 3′-cytidine monophosphate (3′-CMP), one of the potent ribonuclease inhibitors.[35] The experimental data also matched well with the computationally generated partition coefficient values.[52] The results indicated almost similar lipophilicity of these modified nucleosides compared to that of 3′-CMP. Nevertheless, the K_i values suggested better

Table 2 The comparative log *P* values of RNase A inhibitors

Inhibitors	Partition coefficient (SF log $P_{octanol/water}$)[a]	Partition coefficient (A log $P_{octanol/water}$)[b]	Ref.
D (3′-CMP)	−2.11 ± 0.12	−2.00 ± 0.06	28
H	−1.51 ± 0.14	ND	30
I	−1.05 ± 0.10	ND	30
J	−1.67 ± 0.14	−1.69 ± 0.06	28
K	−1.39 ± 0.10	−1.45 ± 0.05	28
2	−2.00 ± 0.20	−1.82 ± 0.10	Present study
4	−1.75 ± 0.22	−1.83 ± 0.10	Present study

[a] Experimentally obtained values. [b] Computationally generated values.

inhibitory properties for **2** and **4** (Table 1) compared to those of 3′-CMP (**D** in Fig. 2).

3. Conclusion

The use of milder reaction conditions led to successful installation of the sulfonic acid group at the 3′-site of pyrimidine nucleosides which are potential mimics of phosphorylated analogues. This new class of modified nucleosides with a relatively high acidic nature is able to perturb the micro-environment of RNase A substantially as reflected by the experimentally determined K_i values. The permeability assay indicated that the lipophilicity values for the representative compound **4** and the nucleotide analogue 3′-CMP were similar. Nevertheless, the former has much better inhibition properties (K_i = 0.96 μM) than 3′-CMP (K_i = 103.0 μM). Docking studies lead us to conclude that strong electrostatic and H-bonding interactions between the sulfonic acid group and the active site (P_1) amino acid residues resulted in a more effective inhibition of the enzyme compared to the previously reported acidic nucleosides. Sulfonic group-modified nucleosides **2** and **4** behaved similar to nucleotides regarding their binding mode and enzyme inhibitory properties against RNase A. Due to the absence of the phosphate group(s), these inhibitors can escape enzyme phosphatase pathways resulting in better stability. This study, therefore, leads to a new series of inhibitors which can efficiently perturb the ribonucleolytic activity of RNase A. Studies on the inhibitory efficiency of these inhibitors with respect to other RNases are currently in progress.

4. Experimental section

4.1. General experimental procedures

All reagents were commercially purchased. Column chromatographic separation was done using silica gel (230–400 mesh). Solvents were dried and distilled following standard procedures. TLC was carried out on precoated plates (Merck silica gel 60, f_{254}) and the spots were visualized with UV light or by charring the plates dipped in 5% H_2SO_4 in MeOH and 5% vanillin in MeOH solutions. ^{1}H-NMR (400 MHz) and ^{13}C-NMR (100 MHz) spectra were recorded on a Bruker NMR spectrometer unless stated otherwise. All ^{1}H and ^{13}C NMR spectra were recorded in $CDCl_3$, DMSO-d_6 and D_2O (using HPLC grade acetonitrile as the internal standard). Chemical shifts are reported in parts per million (ppm, δ scale). DEPT experiments were carried out to identify the methylene carbons. Mass spectroscopy data were obtained from Synapt G2QTof and LCT Micromass mass spectrometers in ESI$^+$ mode. Melting points were determined in open-end capillary tubes and are uncorrected. Bovine pancreatic RNase A, yeast tRNA, 2′,3′-cCMP, 3′-CMP and human serum albumin (HSA) were purchased commercially. UV-Vis measurements were performed using a UV-Vis spectrophotometer (Model Lambda 25). Concentrations of the solutions were estimated spectrophotometrically using the following data: $\varepsilon_{278.5}$ = 9800 M^{-1} cm^{-1} (RNase A)[53] and ε_{268} = 8500 M^{-1} cm^{-1} (2′,3′-cCMP).[35]

4.2. Chemistry

4.2.1. 3′-Deoxy-3′-*S*-[(methoxycarbonyl)methylsulfonyl]-5′-*O*-tritylthymidine 1. Magnesium bis(monoperoxyphthalate) hexahydrate (MMPP) (1.30 g, 2.64 mmol) was added to a solution of 3′-deoxy-3′-*S*-[(methoxycarbonyl)methylthio]-5′-*O*-tritylthymidine[34] (0.50 g, 0.88 mmol) in anhydrous MeOH and the mixture was stirred at room temperature under a N_2 atmosphere. After 8 h, this reaction mixture was concentrated, treated with saturated aqueous $NaHCO_3$ and the solution was washed with EtOAc (2 × 25 mL). Organic layers were separated, dried over anhydrous Na_2SO_4, filtered, and the filtrate was concentrated under reduced pressure. The residue thus obtained was purified over a silica gel column to afford compound **1**[34] (0.41 g, 77%) [eluent: 70% of EtOAc in petroleum ether]. White solid; m.p. 110–112 °C; ^{1}H NMR, 400 MHz ($CDCl_3$, 25 °C, TMS): δ = 9.26 (s, 1H), 7.56 (d, J = 1.2 Hz, 1H), 7.44–7.39 (m, 6H), 7.36–7.23 (m, 9H), 6.27 (t, J = 6.5 Hz, 1H), 4.64 (dd, J = 6.8, 4.0 Hz, 2H), 4.06 (d, J = 15.0 Hz, 1H), 3.96 (d, J = 15.0 Hz, 1H), 3.76 (s, 3H), 3.63 (dd, J = 10.8, 1.7 Hz, 1H), 3.46 (dd, J = 10.7, 2.1 Hz, 1H), 3.07–2.96 (m, 1H), 2.64–2.51 (m, 1H), 1.46 ppm (d, J = 1.0 Hz, 3H); ^{13}C NMR, 100 MHz ($CDCl_3$, 25 °C, TMS): δ = 164.0, 163.2, 150.3, 143.2, 135.3, 128.7, 128.2, 127.7, 111.6, 87.8, 85.1, 64.0, 60.7, 56.8, 53.6, 34.0, 12.0 ppm; HRMS (ESI$^+$), m/z calcd for (M + H)$^+$ $C_{32}H_{33}N_2O_8S$: 605.1958, found: 605.1962.

4.2.2. 3′-Deoxy-3′-*S*-thymidinesulfonic acid 2. NaOH (2 M, 6 mL) was added to a solution of compound **1** (0.11 g, 0.18 mmol) in THF (16 mL). The reaction mixture was stirred for 16 h and the volatile matter was removed under reduced pressure. HCl solution (1 M) was added in portions to the residue and the mixture was stirred until the pH reached 7. The resulting solution was freeze-dried to afford a solid residue which was washed with chilled diethylether (Et_2O) (3 × 15 mL). The crude solid thus obtained was stirred with TFA in DCM (20%, 15 mL) at room temperature. After 4 h, the volatile matter was evaporated to dryness under reduced pressure and the residual liquid was co-evaporated with a mixture of toluene and carbon tetrachloride. The residue was triturated well with chilled Et_2O to obtain solid compound **2** as a white hygroscopic solid (0.032 g, 57%). ^{1}H NMR, 400 MHz (D_2O, 25 °C):

δ = 7.54 (s, 1H), 6.10 (t, J = 6.8 Hz, 1H), 4.54–4.50 (m, 1H), 4.33–4.28 (m, 1H), 3.85–3.81 (m, 1H), 3.73–3.68 (m, 1H), 2.85–2.78 (m, 1H), 2.54–2.50 (m, 1H), 1.77 ppm (s, 3H); ^{13}C NMR, 100 MHz (DMSO-d_6, 25 °C): δ = 164.4, 151.1, 136.6, 110.3, 84.5, 79.0, 62.9, 61.9, 32.6, 12.9 ppm; HRMS (ESI^+), m/z calcd for $(M + H)^+$ $C_{10}H_{15}N_2O_7S$: 307.0591, found: 307.0600.

4.2.3. 1-[5′-*O*-Trityl-3′-deoxy-3′-*S*-(methoxycarbonylmethyl) sulfonyl-β-D-*arabino*-furanosyl]uracil 3. 1-[5′-*O*-Trityl-3′-deoxy-3′-*S*-(methoxycarbonylmethyl)thio-β-D-*arabino*-furanosyl]uracil[28] (0.51 g, 0.89 mmol) was converted to compound **3** (0.45 g, 83%) following the method described for compound **1**.[28] Eluent for column chromatography: 60–80% EtOAc in petroleum ether. White solid; m.p. 100–104 °C; ^{1}H NMR, 400 MHz ($CDCl_3$, 25 °C, TMS): δ = 10.8 (s, 1H), 7.9 (d, J = 8.1 Hz, 1H), 7.48 (d, J = 7.5 Hz, 6H), 7.26 (dt, J = 32.8, 7.3 Hz, 9H), 6.07 (d, J = 4.7 Hz, 1H), 5.26 (d, J = 8.1 Hz, 1H), 5.14 (t, J = 4.6 Hz, 1H), 4.69–4.56 (m, 3H), 4.17 (d, J = 15.3 Hz, 1H), 3.75 (s, 3H), 3.66 (dd, J = 10.6, 3.6 Hz, 1H), 3.49 ppm (dd, J = 10.5, 2.4 Hz, 1H); ^{13}C NMR, 100 MHz ($CDCl_3$, 25 °C, TMS): δ = 165.5, 163.4, 150.8, 143.4, 142.6, 128.8, 128.1, 127.5, 101.3, 87.6, 86.2, 74.6, 72.2, 65.6, 63.4, 57.1, 53.5 ppm; HRMS (ESI^+), m/z calcd for $(M + Na)^+$ $C_{31}H_{30}N_2O_9SNa$: 629.1570, found: 629.1547.

4.2.4. 3′-Deoxy-3′-*S*-*arabino*-uridinesulfonic acid 4. Compound **3** (0.12 g, 0.197 mmol) was converted to compound **4** (0.033 g, 54%) following the method described for compound **2**. White hygroscopic solid; ^{1}H NMR, 400 MHz (D_2O, 25 °C): δ = 7.90–7.67 (m, 1H), 6.10 (t, J = 6.8 Hz, 1H), 5.90–5.87 (m, 1H), 5.07–5.06 (m, 1H), 4.61–4.58 (m, 1H), 4.30–4.28 (m, 1H), 4.07–4.04 (m, 1H), 3.96–3.89 ppm (m, 1H); ^{13}C NMR, 100 MHz (D_2O, 25 °C): δ = 166.3, 152.1, 143.7, 102.2, 86.7, 76.4, 72.0, 67.4, 62.3 ppm; HRMS (ESI^+), m/z calcd for $(M + H)^+$ $C_9H_{13}N_2O_8S$: 309.0393, found: 309.0382.

4.3. Enzyme inhibition

4.3.1. Agarose gel electrophoresis. Inhibition of RNase A was assayed qualitatively by the degradation of tRNA in an agarose gel. In this method, 20 μL of RNase A (2.0 μM) was mixed with 20 μL (0.20 mM) of compounds **2** and **4** to make a final volume of 100 μL and the resulting solutions were incubated for 3 h. 20 μL aliquots of the incubated mixtures were then mixed with 20 μL of tRNA solution (5.0 mg mL^{-1} tRNA, freshly dissolved in RNase-free water) and incubated for another 30 min. Then 10 μL of sample buffer (containing 10% glycerol and 0.025% bromophenol blue) was added to this mixture and 15 μL from each solution was taken and loaded into a 1.1% agarose gel. The gel was run using 0.04 m Tris-Acetic acid-EDTA (TAE) buffer (pH 8.0). The residual tRNA was visualized by ethidium bromide staining under UV light.

4.3.2. Chemical kinetics. The inhibition of RNase A by compounds **2** and **4** was determined individually by a spectrophotometric method as described by Anderson and coworkers.[35] The assay was performed in 0.1 M Mes–NaOH buffer, pH 6.0, containing 0.1 M NaCl using 2′,3′-cCMP as the substrate. The inhibition constants were calculated from the initial velocity data using Lineweaver–Burk plots. For the Lineweaver–Burk plot, the reciprocal of the initial velocity was plotted against the reciprocal of the substrate concentration at a constant inhibitor concentration according to the following equation:

$$\frac{1}{\nu} = \frac{K_m}{V_{max}}\left(1 + \frac{[I]}{K_i}\right)\frac{1}{[S]} + \frac{1}{V_{max}}$$

where ν is the initial velocity, [S] the substrate concentration, [I] the inhibitor concentration, K_m the Michaelis constant, K_i the inhibition constant, and V_{max} the maximum velocity. The kinetics experiments were performed with two fixed inhibitor concentrations and another in the absence of an inhibitor with various substrate (2′,3′-cCMP) concentrations. The slopes from the double reciprocal plot were again plotted against the corresponding inhibitor concentrations to obtain inhibition constants (K_i).

4.3.3. Determination of partition coefficients (log *P*). The shake-flask method was used to determine the partition coefficients of compounds **2** and **4** following a reported procedure.[28,51] Accurately weighed (0.25, 0.50, 1.00 and 2.00 mg) portions of inhibitors **2** and **4** were individually dissolved in 5.0 mL of pH 7.4, 0.01 M phosphate buffer in volumetric flasks. The UV spectrum of each solution was recorded from 600 to 200 nm with a UV-VIS spectrophotometer. The absorbance values of these solutions at the absorption maximum were plotted against their concentrations. A linear relationship indicated that Beer's law was followed. The ε_{max} values of both inhibitors at ~260 nm were calculated. An identical procedure was followed with octanol also. From freshly prepared buffer solutions containing inhibitors, 5.00 mL of each solution were transferred to individual centrifuge cones. To each cone, 5.00 mL octanol was added and the tube was capped tightly. The mixtures were shaken vigorously 50 times and then centrifuged at 2000 rpm for 1 h. The aqueous and organic phases were then separated and the UV spectra of each layer were recorded. The inhibitor concentration in each phase was calculated from its respective absorbance. The P value of the nucleoside was determined using the following expression:

$$P = [c]_{octanol}/[c]_{water}.$$

Consequently, the log P values were also determined and termed $\log P_{octanol/water}$. Thus, the data obtained for the inhibitors were compared with those of 3′-cytidine monophospate (3′-CMP), one of the potent ribonuclease inhibitors.

4.4. Docking studies

Docking experiments were performed to identify the probable binding patterns of the inhibitors with RNase A (1FS3). During this study, the crystal structure of the protein 1FS3 was downloaded from the Protein Data Bank.[49] Water molecules and other ions were subtracted to prepare the PDB file for docking. The 3D structures of compounds **2** and **4** were generated using Sybyl6.92 (Tripos Inc., St Louis, USA) and their energy-minimized conformations were obtained using the MMFF94 force field and MMFF94 charges with a gradient of 0.005 kcal mol^{-1} and 1000 iterations. The FlexX software, which is a part of the

Sybyl suite, was used for docking of the ligands to the protein. The ranking of the generated solutions was performed using a scoring function which estimates the free binding energy (ΔG) of the protein–ligand complex considering various types of molecular interactions.[50] The docked poses were finally visualized using Pymol.[54]

Conflicts of interest

There are no conflicts of interest to declare.

Acknowledgements

The authors are thankful to the Department of Biotechnology, Ministry of Science and Technology, New Delhi for funding (Project No: BT/PR6189/BRB/10/1150/2012). D. Datta thanks the Department of Chemistry and Central Research Facility, Indian Institute of Technology Kharagpur for instrumental facilities.

Notes and references

1 R. T. Raines, *Chem. Rev.*, 1998, **98**, 1045.
2 M. Moussaoui, M. V. Nogues, A. Guasch, T. Barman, F. Travers and C. M. Cuchillo, *J. Biol. Chem.*, 1998, **273**, 25565.
3 H. F. Rosenberg and J. B. Domachowske, *J. Leukocyte Biol.*, 2001, **70**, 691.
4 R. Y. T. Kao, J. L. Jenkins, K. A. Olson, M. E. Key, J. W. Fett and R. Shapiro, *Proc. Natl. Acad. Sci. U. S. A.*, 2002, **99**, 10066.
5 A. A. Makrov and O. N. Ilinskaya, *FEBS Lett.*, 2003, **540**, 15.
6 C. M. Cuchillo, M. V. Nogues and R. T. Raines, *Biochemistry*, 2011, **50**, 7835.
7 G. J. Gleich, D. A. Loegering, M. P. Bell, J. L. Checkel, S. J. Ackerman and D. J. McKean, *Proc. Natl. Acad. Sci. U. S. A.*, 1986, **83**, 3146.
8 D. D. Leonidas, E. Boix, R. Prill, M. Suzuki, R. Turton, K. Minson, G. J. Swaminathan, R. J. Youle and K. R. Acharya, *J. Biol. Chem.*, 2001, **276**, 15009.
9 D. D. Leonidas, R. Shapiro, L. I. Irons, N. Russo and K. R. Acharya, *Biochemistry*, 1999, **38**, 10287.
10 N. Russo and R. Shapiro, *J. Biol. Chem.*, 1999, **274**, 14902.
11 D. E. Holloway, G. B. Chavali, D. D. Leonidas, M. D. Baker and K. R. Acharya, *Biopolymers*, 2009, **91**, 995.
12 N. Doucet, T. B. Jayasundera, M. Simonovic and J. P. Loria, *Proteins*, 2010, **78**, 2459.
13 E. Anslyn and R. Breslow, *J. Am. Chem. Soc.*, 1989, **111**, 4473.
14 J. K. Stowell and T. S. Widlanski, *J. Org. Chem.*, 1995, **60**, 6930.
15 N. Russo, K. R. Acharya and R. Shapiro, *Methods Enzymol.*, 2001, **341**, 629.
16 G. I. Yakovlev, V. A. Mitkevich and A. A. Makarov, *Mol. Biol.*, 2006, **40**, 867.
17 A. G. McLennan, *Pharmacol. Ther.*, 2000, **87**, 73.
18 A. M. Jardine, D. D. Leonidas, J. L. Jenkins, C. Park, R. T. Raines, K. R. Acharya and R. Shapiro, *Biochemistry*, 2001, **40**, 10262.
19 K. Tonan, P. Xu, J. L. Jenkins, A. Russo, R. Shapiro and F. Ni, *Biochemistry*, 2003, **42**, 11137.
20 T. K. Maiti, S. De, S. Dasgupta and T. Pathak, *Bioorg. Med. Chem.*, 2006, **14**, 1221.
21 A. Samanta, D. D. Leonidas, S. Dasgupta, T. Pathak, S. E. Zographos and N. G. Oikonomakos, *J. Med. Chem.*, 2009, **52**, 932.
22 J. Debnath, S. Dasgupta and T. Pathak, *Bioorg. Med. Chem.*, 2009, **17**, 4921.
23 J. Debnath, S. Dasgupta and T. Pathak, *Bioorg. Med. Chem.*, 2009, **17**, 6491.
24 A. Samanta, S. Dasgupta and T. Pathak, *Bioorg. Med. Chem.*, 2011, **19**, 2478.
25 N. Thiyagarajan, B. D. Smith, R. T. Raines and K. R. Acharya, *FEBS J.*, 2011, **278**, 541.
26 J. Debnath, S. Dasgupta and T. Pathak, *Chem. – Eur. J.*, 2012, **18**, 1618.
27 V. Parmenopoulou, D. S. M. Chatzileontiadou, S. Manta, S. Bougiatioti, P. Maragozidis, D. Gkaragkouni, E. Kaffesaki, A. L. Kantsadi, V. T. Skamnaki, S. E. Zographos, P. Zounpoulakis, N. A. A. Balatsos, D. Komiotis and D. D. Leonidas, *Bioorg. Med. Chem.*, 2012, **20**, 7184.
28 D. Datta, S. Dasgupta and T. Pathak, *ChemMedChem*, 2014, **9**, 2138.
29 D. S. M. Chatzileontiadou, V. Parmenopoulou, S. Manta, A. L. Kantsadi, P. Kylindri, M. Griniezaki, F. Kontopoulou, A. Telopoulou, H. Prokova, D. Panagopoulos, E. Boix, N. A. A. Balatsos, D. Komiotis and D. D. Leonidas, *Bioorg. Chem.*, 2015, **63**, 152.
30 D. Datta, S. Dasgupta and T. Pathak, *ChemMedChem*, 2016, **11**, 620.
31 D. Datta, P. Mondal, S. Dasgupta and T. Pathak, *ChemistrySelect*, 2017, **2**, 2106.
32 A. Kayet, D. Datta, A. Das, S. Dasgupta and T. Pathak, *Bioorg. Med. Chem.*, 2018, **26**, 455.
33 D. G. Herries, A. P. Mathias and B. R. Rabin, *Biochem. J.*, 1962, **85**, 127.
34 D. Datta, A. Samanta, S. Dasgupta and T. Pathak, *Bioorg. Med. Chem.*, 2013, **21**, 4634.
35 (*a*) D. G. Anderson, G. G. Hammes and F. G. Walz, *Biochemistry*, 1968, **7**, 1637; (*b*) C. L. Jenkins, N. Thiyagarajan, R. Y. Sweeney, M. P. Guy, B. R. Kelemen, K. R. Acharya and R. T. Raines, *FEBS J.*, 2005, **272**, 744.
36 K. Iwahashi, K. Nakamura, Y. Mitsui, K. Ohgi and M. Irie, *J. Biochem.*, 1981, **90**, 1685.
37 Y. Mizuno, C. Kaneko and Y. Oikawa, *J. Org. Chem.*, 1974, **39**, 1440.
38 P. H. C. Mundill, R. W. Fries, C. Woenckhaus and B. V. Plapp, *J. Med. Chem.*, 1981, **24**, 474.

39 C. Glemarec, R. C. Reynolds, P. A. Crooks, J. A. Maddry, M. S. Akhtar, J. A. Montgomery, J. A. Secrist III and J. Chattopadhyaya, *Tetrahedron*, 1993, **49**, 2287.
40 M. Xie and T. S. Widlanski, *Tetrahedron Lett.*, 1996, **37**, 4443.
41 Z. Huang and S. A. Benner, *J. Org. Chem.*, 2002, **67**, 3996.
42 J. P. Guthrie, *Can. J. Chem.*, 1978, **56**, 2342.
43 Oligomers of vinylsulfonic acid (OVS) were found to be efficient competitive inhibitors of RNase A with a very low K_i value (11 pM), see: B. D. Smith, M. B. Soellner and R. T. Raines, *J. Biol. Chem.*, 2003, **278**, 20934.
44 M. D. Dutov, O. V. Serushkina, S. A. Shevelev, K. A. Lyssenko and A. Konstantin, *Mendeleev Commun.*, 2007, **17**, 347.
45 W. Qian, J.-E. Park, F. Liu, K. S. Lee and T. R. Burke Jr., *Bioorg. Med. Chem.*, 2013, **21**, 3996.
46 G. A. El-Hiti, *Sulfur Rep.*, 2001, **22**, 217.
47 Y. Joyard, C. Papamicael, P. Bohn and L. Bischoff, *Org. Lett.*, 2013, **15**, 2294.
48 L. M. Lima and E. J. Barreiro, *Curr. Med. Chem.*, 2005, **12**, 23.
49 M. H. Berman, J. Westbrook, Z. Feng, G. Gilliland, T. N. Bhat, H. Weissig, I. N. Shindyalov and P. E. Bourne, *Nucleic Acids Res.*, 2000, **28**, 235.
50 M. Rarey, B. Kramer, T. Lengauer and G. Klebe, *J. Mol. Biol.*, 1996, **261**, 470.
51 A. P. Cheung and D. Kenney, *J. Chromatogr.*, 1990, **506**, 119.
52 I. V. Tetko and V. Y. Tanchuk, *J. Chem. Inf. Comput. Sci.*, 2002, **42**, 1136.
53 M. Sela and C. B. Anfinsen, *Biochim. Biophys. Acta*, 1957, **24**, 229.
54 W. L. DeLano, *The PyMOL Molecular Graphics System*, DeLano Scientific, San Carlos, CA, USA, 2006; http://pymol.sourceforge.net/.